Weinstein, S. W., & Szyjewics, J. (1971) *Am. J. Physiol. 227*, 171–177.

Wemmer, D., Wade-Jardetzky, N., Robin, E., & Jardetzky, O. (1982) *Biochim. Biophys. Acta 720*, 281–287.

Wikman-Coffelt, J., Sievers, R., Coffelt, R. S., & Parmley, W. W. (1983) *Am. J. Physiol. 245*, H354–H362.

Yahaya, H., Chan, L., Freeman, D., Holloway, P., & Ross, B. (1984) *Clin. Sci. 66*, 35p.

Metal Ion Binding Properties of Hen Ovalbumin and S-Ovalbumin: Characterization of the Metal Ion Binding Site by ^{31}P NMR and Water Proton Relaxation Rate Enhancements†

Warren J. Goux* and P. N. Venkatasubramanian

Department of Chemistry, The University of Texas at Dallas, Richardson, Texas 75083-0688

Received May 22, 1985

ABSTRACT: In this study, water proton relaxation rate (PRR) enhancements have been used to characterize the binding of metal ions to native ovalbumin, ovalbumin in which phosphate has been enzymatically cleaved from one or both of the two protein phosphoserines, and a heat-stabilized form of the protein (S-ovalbumin). With Scatchard plots constructed from water PRR enhancements, it was found that native ovalbumin and S-ovalbumin had one strong binding site for Mn^{2+} ion ($K_D \simeq 6.0 \times 10^{-4}$ M). Alkaline phosphatase treated ovalbumin, a protein having a single phosphoserine, had one Mn^{2+} binding site of slightly weaker affinity ($K_D \simeq 8.3 \times 10^{-4}$ M), while acid phosphatase treated ovalbumin, a dephosphorylated protein, had two much weaker Mn^{2+} ion binding sites ($K_D \simeq 1.3 \times 10^{-3}$ M). Competitive binding studies on the native protein suggested that Zn^{2+} ion competes with Mn^{2+} for the single strong-affinity site ($K_D \simeq 6.1 \times 10^{-3}$ M) while Mg^{2+} and Ca^{2+} do not. In a second set of experiments, the paramagnetic contribution to the ^{31}P spin–lattice (T_{1P}) and spin–spin (T_{2P}) relaxation times at three separate magnetic field strengths was measured. Correlation times τ_c characterizing Mn^{2+}–^{31}P dipolar relaxation were estimated from the ratios of T_{1P}/T_{2P} at a single field and from the ratios of spin–lattice relaxation rates at three different field strengths. The correlation times so obtained, ranging from about 0.7 to 7.7 ns at the three field strengths, were used in calculating distances from the bound Mn^{2+} ion to the phosphoserines of native ovalbumin, S-ovalbumin, and alkaline phosphatase treated ovalbumins. It was determined that the phosphate of phosphoserine-68 was 5.95 ± 0.26 and 6.29 ± 0.18 Å from the Mn^{2+} in the native and alkaline phosphatase treated protein, respectively, and 6.99 ± 0.30 Å away from the Mn^{2+} in S-ovalbumin. The phosphate of phosphoserine-344 was determined to be 5.31 ± 0.20 and 5.75 ± 0.10 Å from the Mn^{2+} ion in native ovalbumin and S-ovalbumin, respectively. The ^{13}C nucleus of [1-^{13}C]galactose enzymatically transferred to the nonreducing end of the ovalbumin oligosaccharide chain was not found to be significantly relaxed by Mn^{2+} bound to the protein, even at 1:1 stoichiometric ratio of metal:protein. Using this, we estimate the nonreducing terminal of the ovalbumin oligosaccharide to be at least 39 Å from the metal ion binding site on the protein.

Hen ovalbumin is a soluble glycoprotein (M_r 42 700) having a single carbohydrate chain covalently linked to the nitrogen amide of an asparagine residue (Taborsky, 1974; Nisbet et al., 1981). Although the tertiary structure has not been determined by X-ray crystallography, the complete primary sequence of its 348 amino acid residues is known (Nisbet et al., 1981; McReynolds et al., 1978). The protein has been shown to be heterogeneous, both with respect to its attached carbohydrate chain (Atkinson et al., 1981; Tai et al., 1975; Narashiman et al., 1980) and with respect to the degree of phosphorylation of two of its serine side chains (Linderstrom-Lang & Ottesen, 1949). Heterogeneity of the protein due to varying degrees of phosphorylation may be removed by ion-exchange chromatography (Rhodes et al., 1958). The major protein component has two phosphoserines present, while minor components bear only one of the two phosphoserines per protein equivalent. When the native protein is warmed under alkaline conditions, a conformational change takes place and native ovalbumin is converted to a more heat-resistant form (S-ovalbumin) (Smith & Black, 1968a,b; Donovan & Mapes, 1976). The S form of the protein is hydrodynamically more compact and has a greater number of tritratable groups exposed to the protein surface (Nakamura et al., 1981, 1980; Nakamura & Masuko, 1981; Kint & Tomimatsu, 1979). Although the functional significance of ovalbumin is not known, it has for some time been thought responsible for metal ion transport and storage (Taborsky, 1974). However, only the Mg^{2+} binding characteristics of the protein have been studied (Vogel & Bridger, 1982).

In this study, water proton relaxation rate (PRR) enhancements and ^{31}P NMR relaxation rate data are used to determine the metal ion binding properties, titratability of the two phosphoserines, and distances from protein-bound paramagnetic Mn^{2+} to each of the two phosphoserines of native ovalbumin and its conformational variant, S-ovalbumin. In an attempt to determine changes in Mn^{2+} ion–carbohydrate

---

† This work was supported by Grant AT-885 from the Robert A. Welch Foundation and by BRSG S07 RR07133 awarded by the Biomedical Research Support Grant Program, Division of Research Resources, National Institutes of Health.

* Author to whom correspondence should be addressed.

0006-2960/86/0425-0084\$01.50/0 © 1986 American Chemical Society

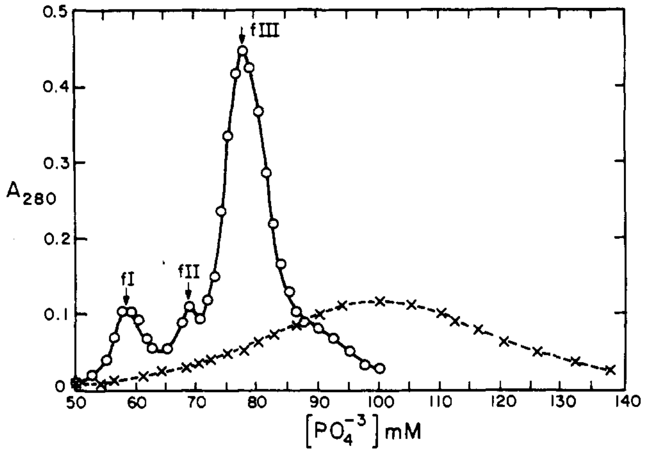

FIGURE 1: DEAE-cellulose ion-exchange chromatography at pH 7.0 of 200 mg of commercial ovalbumin (○) and 150 mg of S-ovalbumin (×) prepared from chromatographically purified fraction III (fIII) protein. In the case of chromatography of the native ovalbumin, the protein was eluted from the column (2.5 × 40 cm) by linearly increasing the sodium phosphate buffer concentration from 10 to 100 mM over a total gradient volume of 2 L. For chromatography of S-ovalbumin, the sodium phosphate buffer concentration was linearly increased from 25 to 200 mM over a total gradient volume of 2 L. Ten-milliliter protein fractions were collected in both cases. The column flow rate varied between 20 and 60 mL/h.

distances brought about by changes in protein conformation, [1-^{13}C]galactose was enzymatically attached to the nonreducing terminal end of the ovalbumin oligosaccharide chain, and attempts were made to determine ^{31}C–Mn^{2+} distances for both native ovalbumin and S-ovalbumin.

EXPERIMENTAL PROCEDURES

Materials, Sample Preparations, and Purifications. Ovalbumin was obtained from Sigma Chemical Co. (St. Louis, MO). A variety of batches of the protein (grade V) all gave identical ^{31}P NMR spectra. These batches chromatographed slightly differently on DEAE-cellulose with respect to the relative proportions of the protein subfractions (see below). All batches gave a single band on sodium dodecyl sulfate (NaDodSO$_4$)–acrylamide gel. Alkaline phosphatase (*Escherichia coli*), acid phosphatase (potato), α-mannosidase (jack bean), *N*-acetylglucosaminidase (jack bean), galactosyltransferase (bovine colostrum), and galactoase-4′-epimerase (*E. coli*) were obtained from the same source and were used without further purification.

Commercially obtained hen ovalbumin was purified on DEAE-cellulose. This method of purification differs from that previously reported by Rhodes et al. (1958) for the chromatographic purification of ovalbumin from egg white on carboxylmethylcellulose (CM-cellulose). Typically, by our method, 0–2 g of the commercial protein was dissolved in 10 mM sodium phosphate buffer, pH 7.0, and applied to a 2.5 × 40 cm column of DEAE-cellulose, previously equilibrated with the same buffer. The protein was eluted from the column with a linear concentration gradient of sodium phosphate buffer, where the phosphate concentration was varied from 10 to 100 mM (1–2 L total volume). The flow rate of the column varied between 20 and 60 mL/h. Ten-milliliter fractions were collected. A typical chromatograph is shown in Figure 1. Three major protein fractions are observed to successively elute from the column with linearly increasing phosphate buffer concentration. Although the separation of crude ovalbumin into three distinct subfractions has not previously been reported with DEAE-cellulose as a chromatography medium, the relative proportions of protein subfractions present are such so as to make likely the correspondence of fI through fIII with subfractions A$_3$ through A$_1$ obtained by CM-cellulose chromatography (Rhodes et al., 1958). All subfractions migrated on (NaDodSO$_4$)–acrylamide gels identically with one another and also identically with the unchromatographed protein. ^{31}P NMR spectra of fIII were identical in all respects with spectra of the unfractionated protein, showing two resonances previously assigned to the phosphates of phosphoserines-68 and -344 (Vogel & Bridger, 1982). Spectra of purified fI and fII were identical, both proteins lacking the resonance previously assigned to phosphoserine-344. Metal ion binding properties of fIII were found to be identical with those of the commercially obtained protein in all experiments reported.

S-Ovalbumin was prepared from unchromatographed commercial or fraction III (fIII) ovalbumin by heating a 2 mM aqueous, unbuffered protein solution, pH 10.0, to 56 °C for 38 h (Kint & Tomimatsu, 1979). Total conversion to the S form of the protein was checked by differential scanning calorimetry using a Perkin-Elmer DSC-2 differential scanning calorimeter and 20-μL sample cells. In agreement with the findings of Donovan & Mapes (1976), conversion of the native protein to the S form increased the denaturation temperature from 84 ± 0.5 to 92 ± 0.5 °C.

Chromatography of S-ovalbumin on DEAE-cellulose (Figure 1) shows that the protein elutes from the column as a broad peak, within which no subfractions are resolvable. A similar loss of resolvable S-ovalbumin subfractions has previously been detected by using isoelectric focusing techniques (Nakamura et al., 1980). The 80.76-MHz ^{31}P NMR spectrum was identical with that of commercially obtained or chromatographically purified ovalbumin.

Ovalbumin samples used for ^{31}P NMR and metal ion binding studies were prepared by concentrating pooled chromatographic fractions with an Amicon (Lexington, MA) ultrafiltration apparatus equipped with a YM-5 membrane. Ovalbumin concentrations were measured spectrophotometrically by using the known molar extinction coefficient (Tomimatsu, 1965). The pH of protein and buffered solutions were measured on a Radiometer PHM62 pH meter equipped with a glass electrode. When necessary, the pH was adjusted with 0.1 N NaOH or HCl. The pH values reported for ^{31}P NMR samples containing 20% D$_2$O (99.8%) are reported as uncorrected pH values, where the deuterium ion activity has not been taken into account (Glasoe & Long, 1960). In the case of metal ion binding studies, microliter quantities of unbuffered aqueous solutions containing the paramagnetic metal ion of interest were added to the concentrated protein solution. The concentrations of metal ion in dilute aqueous solutions were determined by atomic absorption against calibration standards diluted to 0.5–4.0 ppm.

Enzymatically Modified Ovalbumins. [1-^{13}C]Galactose was attached to the nonreducing *N*-acetylglucosamine of the single ovalbumin oligosaccharide chain as previously described (Goux et al., 1982). In a separate set of experiments, native ovalbumin was treated with glycosidases in a manner previously described by Berman et al. (1981). A carbohydrate analysis of the dialysate carried out by using phenol–sulfuric acid (Dubois et al., 1956) showed that approximately 0.8 mol of total hexose was removed per mole of protein. Both native and modified proteins were then dialyzed against several changes of tris(hydroxymethyl)aminomethane (Tris) buffer, pH 7.8.

Native ovalbumin was partially or completely dephosphorylated by treatment with *E. coli* alkaline phosphatase or potato acid phosphatase according to reaction conditions specified by Vogel & Bridger (1982).

Metal Ion Binding Studies. The binding constants of paramagnetic metals to ovalbumin were determined by measuring the water proton relaxation rate (PRR) enhancement as a function of the fraction of metal bound to the protein. Here, water PRR enhancement ϵ^* is defined as

$$\epsilon^* = \frac{1/T_{1\mathrm{P}}^*}{1/T_{1\mathrm{P}}} = \frac{1/T_1^* - 1/T_{1(0)}^*}{1/T_1 - 1/T_{1(0)}} \qquad (1)$$

where $1/T_1$ is the relative rate in the presence of paramagnetic ion and $1/T_{1(0)}$ is the correspnoding rate in its absence. The terms with asterisks denote the presence of protein. The terms in $1/T_{1\mathrm{P}}$ then represent the paramagnetic contribution to the water proton relaxation rate.

As described by Mildvan & Cohn (1963), two types of titrations were carried out. In the first of these types, a constant concentration of paramagnetic metal is titrated with protein. In the limit of high protein concentrations

$$1/\epsilon^* = (K_\mathrm{D}/\epsilon_\mathrm{b})(1/P_\mathrm{t}) + 1/\epsilon_\mathrm{b} \qquad (2)$$

where ϵ_b is the water PRR enhancement arising from the binary metal–protein complex at the site of strongest binding, K_D is the metal–protein dissociation constant for the strongest binding site, and P_t is the total protein concentration. A plot of $1/\epsilon^*$ vs. $1/P_\mathrm{t}$, in the limit of high protein concentrations, yields a straight line from which ϵ_b and K_D may be determined (see Figure 3A).

In the second type of experiment, water PRR enhancement is measured as a function of increasing paramagnetic metal ion concentrations, while the total amount of protein is held constant. Once ϵ_b is known, the amount of paramagnetic metal ion free and bound to the protein may be determined by using data from both titrations (Mildvan & Cohn, 1963):

$$M_\mathrm{f} = [(\epsilon_\mathrm{b} - \epsilon^*)/(\epsilon_\mathrm{b} - 1)]M_\mathrm{t} \qquad (3\mathrm{A})$$

$$M_\mathrm{b} = [(\epsilon^* - 1)/(\epsilon_\mathrm{b} - 1)]M_\mathrm{t} \qquad (3\mathrm{B})$$

Here, M_f and M_b represent the concentrations of paramagnetic ion free in solution and bound to the protein. M_t is the sum of M_f and M_b. The total number of different types of binding sites and an expression for the average dissociation constants for each type of site may be found by treating such data in the form of a Scatchard plot (Scatchard, 1949).

Binding of diamagnetic metals to the protein may be studied by water PRR enhancements if the diamagnetic metal ion competes for a binding site with a paramagnetic ion. In this case, rearrangement of mass equilibria relationships yields the expression (Granot & Kearns, 1982)

$$\alpha - 1 = (\epsilon_\mathrm{b} - \epsilon^*)/(\epsilon^* - 1) = \beta/\Delta\theta - 1/\Delta \qquad (4)$$

where β is the concentration ratio of the total diamagnetic ion to total protein, θ is the concentration of bound diamagnetic ion to total protein, Δ is the ratio of the dissociation constant of the diamagnetic ion–protein complex to that of the paramagnetic ion–protein complex, and ϵ^* is the PRR enhancement in the presence of added diamagnetic ion. Over a limited range of protein to diamagnetic metal ion concentrations, θ remains nearly constant and a plot of $\alpha - 1$ vs. β yields a linear plot from which the dissociation constant of the diamagnetic metal ion–protein complex may be determined.

Spin–lattice relaxation times used for calculating water PRR enhancements were measured by an inversion–recovery pulse sequence at 60 MHz using a Varian A-60 electromagnet and a Spin-Lock, Ltd. CPS-2 pulse programmer system. The free induction decay was displayed in absolute value mode on an oscilloscope, and inversion–recovery rates were estimated by the delay time between the 180° and 90° pulse that minimized the signal intensity. Temperature into the probe was controlled by using a flow of dry air passed through a set of heat exchange coils immersed in a temperature-regulated bath. Unless otherwise specified, all measurements were made at 30 ± 1 °C. Samples were positioned in the probe in 5-mm sample tubes. All samples were prepared to a total volume of 0.1 mL.

^{31}P NMR Measurements. High-field ^{31}P NMR measurements were made on unbuffered ovalbumin solutions maintained at 30 ± 1 °C, unless otherwise stated. Prior to spectral acquisition, protein samples were treated with Chelex 100 (Bio-Rad Laboratories, Richmond, CA) or extensively dialyzed in order to remove trace metal ions, concentrated by ultrafiltration, and then diluted with D_2O (20% total by volume), for the purpose of maintaining the spectrometer field-frequency lock. Samples were run in the presence of proton decoupling on a JEOL-FX200 spectrometer (46.85 kG, 80.76-MHz ^{31}P resonant frequency), on a JEOL-FX90 spectrometer located at North Texas State University, Denton, TX (21.02 kG, 36.22-MHz ^{31}P resonant frequency), or on a Nicolet NTC 300 spectrometer (70.48 kG, 121.46-MHz ^{31}P resonant frequency) equipped with a Nicolet 1280 data acquisition system and a 239A pulse programmer located at The University of Texas Health Science Center, Dallas, TX. All spectrometers operated in the Fourier transform mode. In the case of spectra acquired at 36.22 and 121.46 MHz, samples were contained in 12-mm sample tubes. Samples run at 80.76 MHz were contained in 15-mm sample tubes with an inner coaxial insert containing the trisodium salt of methylenediphosphonic acid, which was used as an external chemical shift reference. Initial ^{31}P NMR spectra of ovalbumin above pH 7 revealed marked broadening of resonances at protein concentrations much above 3 mM. Such broadening of resonances may arise from decreased spin–spin relaxation times resulting from protein aggregation (Norton & Allerhand, 1977). Spectra that are reported herein were acquired at protein concentrations equal to or less than 3 mM.

In Mn^{2+} titration experiments, microliter amounts of a 10 mM $\mathrm{MnSO_4}$ solution were added to concentrated ovalbumin samples at pH 7.8, and spin–lattice and spin–spin relaxation times were measured (T_1 and T_2, respectively). T_1 values were measured for ^{31}P resonances at 36.22 and 80.76 MHz by the inversion–recovery method (Vold et al., 1968) and at 121.46 MHz by progressive saturation (Freeman & Hill, 1971). T_2 values were either measured by using a Carr–Purcell–Meiboom–Gill (CPMG) sequence (Carr & Purcell, 1954; Meiboom & Gill, 1958) or estimated from the measured line widths ($W_{1/2} = 1/\pi T_2$, where $W_{1/2}$ is the resonance line width measured at half-height). Errors of ±10%, ±15%, and ±25%, respectively, were assumed in inversion–recovery, CPMG, and line width measurements, on the basis of the precision obtained upon repeated measurements. Temperatures were measured on ovalbumin samples that had been preequilibrated in the sample probe for 30 min prior to spectral acquisition.

Analysis of data for NMR relaxation brought about by the presence of paramagnetic metal ions has been previously discussed in detail (James, 1975). According to the Luz–Meiboom and Swift–Connick equations (Luz & Meiboom, 1964; Swift & Connick, 1962), the paramagnetic ion contribution to the spin–lattice and spin–spin relaxation rates ($1/T_{1\mathrm{P}}$ and $1/T_{2\mathrm{P}}$) can be related to the relaxation times of nuclei of the ligand in the metal complex ($T_{1\mathrm{M}}$ and $T_{2\mathrm{M}}$), according to the relations

$$1/T_{1\mathrm{P}} = f/(T_{1\mathrm{M}} + \tau_\mathrm{M}) + \mathrm{OS} \qquad (5\mathrm{A})$$

$$1/T_{2P} = f/(T_{2M} + \tau_M) + \mathrm{OS} \qquad (5B)$$

where τ_M is the residence lifetime of the metal ion–ligand complex and OS is the outer-sphere contribution to T_{1P} and T_{2P} arising from metal ion distant from the ligand binding site. For ligands that bind in the near vicinity of the metal ion, this outer-sphere contribution is usually quite small (James, 1975), and in the present study, it has been neglected. If T_{1P} and T_{2P} demonstrate a field dependence, then $\tau_M < T_{1M}$, T_{2M}, and these latter relaxation times may be approximated by normalized values $1/fT_{1P}$ and $1/fT_{2P}$, where f, the fraction of ligand bound to the metal ion, is determined from knowledge of the binary metal ion–protein dissociation constant. One may relate relaxation rates of the nuclei of the ligand to distance from the paramagnetic ion through the simplified forms of the Solomon–Bloembergen equations (Solomon, 1955; Bloembergen, 1957)

$$1/T_{1M} = \frac{C}{r^6}\left(\frac{3\tau_c}{1 + \omega_I^2\tau_c^2} + \frac{7\tau_c}{1 + \omega_S^2\tau_c^2}\right) \qquad (6A)$$

$$1/T_{2M} = \frac{C}{2r^6}\left(4\tau_c + \frac{3\tau_c}{1 + \omega_I^2\tau_c^2} + \frac{13\tau_c}{1 + \omega_S^2\tau_c^2}\right) + \mathrm{SF} \qquad (6B)$$

where C is a collection of constants, r is the distance between the paramagnetic center and the nucleic of interest, ω_I is $2\pi\nu_I$, where ν_I is the resonance frequency in hertz, $\omega_S = 657\omega_I$, τ_c is the correlation time arising from dipolar relaxation, and SF is a scalar function, dependent upon scalar coupling between the unpaired electron on the metal ion and the nuclei on the ligand. An estimation of correlation time, τ_c, may be obtained either by taking the ratio of $1/T_{1P}$ and $1/T_{2P}$ at a single field or by taking the ratios of $1/T_{1P}$ values obtained at different fields. Because of the possible contribution of the scalar function to $1/T_{2P}$, leading to erroneously large τ_c values, the latter procedure for estimation of τ_c is preferred (Nowak et al., 1973). Once an estimate of τ_c has been made, the distance to the paramagnetic ion may be made directly from eq 6A. Because of the r^6 dependence, errors of 100% in the estimation of τ_c only result in a 12% error in calculated values of r.

RESULTS

pK_a's of Phosphoserines of Ovalbumin Proteins. Vogel and Bridger have previously shown there to be two resolvable resonances in ^{31}P NMR spectra of native ovalbumin (Vogel & Bridger, 1982). The resonances at low and high field were assigned by these workers to the phosphates of phosphoserines-68 and -344, respectively. When the native protein was treated with alkaline phosphatase, they observed that the phosphate of the more solvent-accessible phosphoserine-344 was cleaved, leaving a protein monophosphorylated at phosphoserine-68. On the other hand, native ovalbumin treated with acid phosphatase under slightly acidic conditions yielded a completely dephosphorylated protein. When native ovalbumin is heated to 56 °C at pH 10 for 36 h, the protein is transformed to a modified protein (S-ovalbumin) that has a secondary structure different from that of either the native protein or a denatured protein (Smith & Black, 1968a,b; Donovan & Mapes, 1976; Nakamura et al., 1981, 1980; Nakamura & Masuko, 1981; Kint & Tomimatsu, 1979). Figure 2 shows the pH dependence of the chemical shifts of the ^{31}P resonances of the phosphoserines of commercial ovalbumin, S-ovalbumin prepared from the commercial sample, and alkaline phosphatase treated commercial ovalbumin.

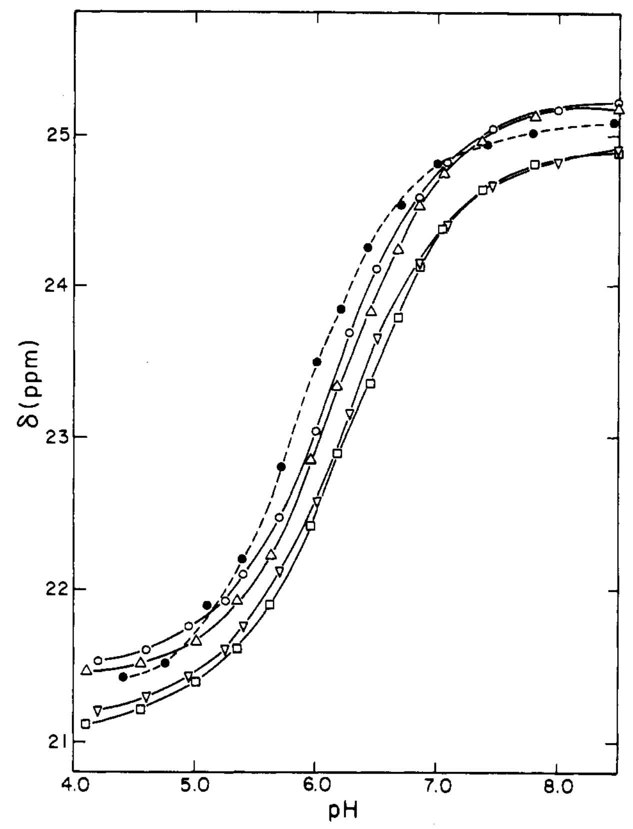

FIGURE 2: pH dependence of the chemical shifts of the single phosphoserine of alkaline phosphatase treated ovalbumin (●), phosphoserine-68 of native ovalbumin (○) and S-ovalbumin (△), and phosphoserine-344 of native ovalbumin (▽) and S-ovalbumin (□). Lines drawn through the points represent calculated best fits to experimental data. The best-fit pK_a's for phosphoserines-68 and -344 of native ovalbumin and S-ovalbumin fall within the range 6.20 ± 0.05. The best-fit pK_a of phosphoserine-68 of the alkaline phosphatase treated protein is 5.60 ± 0.15.

Throughout their titration range, no changes in ^{31}P line widths were observed, indicating that both protonated and deprotonated forms of phosphoserine are in rapid exchange on the NMR time scale. Such behavior is typical of titrating groups of proteins and model compounds, where the titrating group is fully exposed to the solvent (Vogel et al., 1982). A nonlinear best fit to the titration data yielded 6.16 ± 0.03, 6.19 ± 0.06, and 5.60 ± 0.15 for the pK_a's of phosphoserine-68 of commercial ovalbumin, S-ovalbumin, and alkaline phosphatase treated ovalbumin. Within experimental error, the best-fit values for phosphoserine-344 of native and S-ovalbumin were identical with those of phosphoserine-68 (6.22 ± 0.03 and 6.23 ± 0.05, respectively, for native and S forms of the proteins).

Manganese Binding by Ovalbumin Proteins. The binding of manganese to ovalbumin proteins was studied at pH 7.8 and 30 °C with water PRR enhancements. In the first type of experiment, a fixed concentration of Mn^{2+} was titrated with protein, while the total volume of the sample mixture was held constant (type I titration). The enhancement ϵ^* at any fixed protein concentration is the weighted average of enhancement for each type of binding site present (Mildvan & Cohn, 1963). In the limit of high protein concentration $1/\epsilon^*$ values linearly with $1/p_t$ (eq 2). The y intercept of such a linear plot yields the reciprocal of the enhancement of the binary Mn^{2+}–protein complex, ϵ_b, for the strongest binding site, and the ratio of slope to intercept yields the binary Mn^{2+}–protein dissociation constant, K_D, for the site of strongest binding. A double-reciprocal plot, as described, is shown in Figure 3A for ovalbumin, S-ovalbumin, and phosphatase treated ovalbumins. Lines shown

Table I: Binding Parameters Obtained from Water Proton Relaxation Rate Enhancements for the Binding of Mn^{2+} to Ovalbumin Proteins[a]

protein sample	ϵ_b[b]	n[c]	K_D[c] ($\times 10^4$ M)	K_D[b] ($\times 10^4$ M)
ovalbumin	10.68 ± 0.23	1.08 ± 0.12	5.47 ± 1.28	5.29 ± 0.18
S-ovalbumin	11.17 ± 0.31	1.07 ± 0.11	6.05 ± 1.38	6.32 ± 0.34
alkaline phosphatase treated ovalbumin	12.94 ± 0.37	1.04 ± 0.16	9.34 ± 2.87	8.31 ± 0.31
acid phosphatase treated ovalbumin	15.44 ± 0.14	1.79 ± 0.17	12.88 ± 1.62	13.05 ± 0.23

[a] All ovalbumin sample were obtained from unchromatographed commercial ovalbumin. In all cases, the results are within experimental error of those obtained with chromatographically pure fIII. All data were acquired in 50 mM Tris buffer, pH 7.8 at 30 °C. [b] Obtained from type I titration data. [c] Obtained from data of type I and type II titrations, plotted in the form of a Scatchard plot.

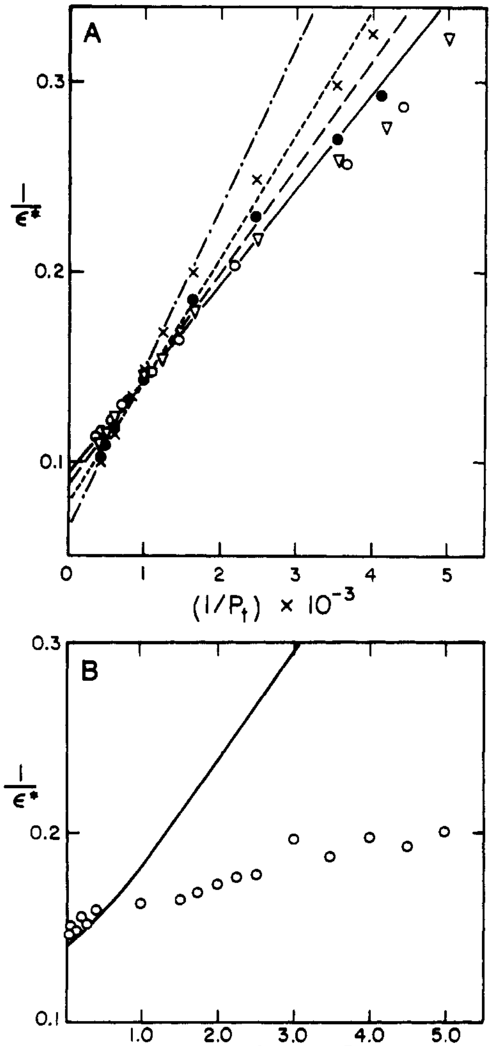

FIGURE 3: Water PRR enhancement data for the Mn^{2+}–ovalbumin system, pH 7.8, at 30 °C in 50 mM Tris buffer. (A) Type I titration in which 0.2 mM $MnSO_4$ was titrated with commercial ovalbumin (○), S-ovalbumin prepared from the commercial protein (▽), and commercial ovalbumin following treatment with *E. coli* alkaline phosphatase (●) or potato acid phosphatase (×). The data are plotted as the reciprocal enhancement ($1/\epsilon^*$) vs. reciprocal total protein concentration ($1/p_t$). Lines in the figure represent linear least-squares best fits to experimental data for native ovalbumin (—), acid phosphatase treated ovalbumin (–·–), alkaline phosphatase treated ovalbumin (---), and S-ovalbumin (– –) at high protein concentrations (greater than 0.5 mM). (B) Type II titration in which 0.9 mM commercial ovalbumin was titrated with $MnSO_4$. Experimental data points are plotted as reciprocal enhancement ($1/\epsilon^*$) vs. total manganese concentration. The solid line represents calculated $1/\epsilon^*$ values assuming a single binding site with ϵ_b and K_D values extrapolated from the type I titration and summarized in Table I.

in the figure represent least-squares fits to data obtained above 0.5 mM protein. More dilute protein samples gave data that deviated substantially from calculated best-fit lines. This deviation arises primarily from the approximations made in the derivation of eq 2 (the linearity of $1/\epsilon^*$ vs. $1/p_t$ plots holds only at high protein concentrations). Parameters determined from least-squares fits to the type I titration data are summarized in Table I.

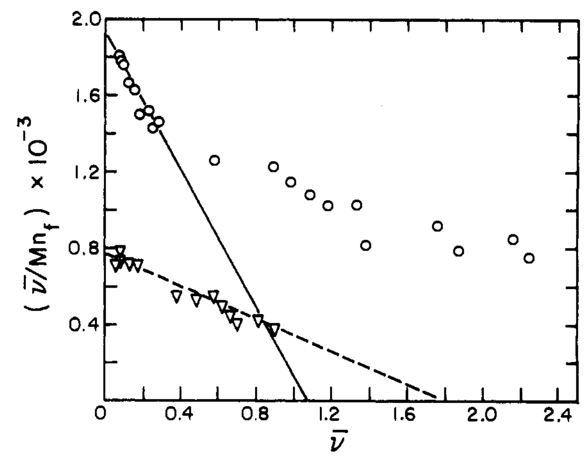

FIGURE 4: Scatchard plot showing the fraction of protein having bound Mn^{2+} (ν) vs. the ratio of ν to Mn^{2+} free in solution. Experimental data points were calculated from type I andd type II water PRR enhancement data for native (○) and acid phosphatase treated ovalbumin (▽), assuming ϵ_b values extrapolated from type I titration and summarized in Table I.

In a second type of experiment, a fixed concentration of protein was titrated with Mn^{2+}, while the total sample volume was held constant (type II titration). As demonstrated previously, extrapolation of the enhancement data to zero Mn^{2+} concentration yields a lower limit for ϵ_b, the enhancement of the binary metal–protein complex having the strongest binding affinity (Mildvan & Cohn, 1963). Figure 3B shows typical data obtained for a type II titration of commercial ovalbumin with Mn^{2+}, with the total protein concentration being held fixed. The solid curve in the figure was calculated by assuming a single binding site and using ϵ_b and K_D values obtained from the type I titration (Table I). At Mn^{2+} concentrations much above 0.5 mM, the calculated curve drastically deviates from the experimental data. The much larger values of ϵ^* observed at high Mn^{2+} concentrations must arise from additional contributions to ϵ^* from weaker secondary binding sites.

Once ϵ_b has been determined from a type I titration, the fraction of protein occupied with Mn^{2+} (ν) may be determined (see eq 3A and 3B). The data may be plotted in the form of a Scatchard plot as shown in Figure 4, where type I and type II titration data for commercial ovalbumin and acid phosphatase treated commercial ovalbumin are presented. The x intercept of least-squares curves generated from the data yields the total number of binding sites while the y intercept yields a weighted average of association constants for the metal–protein complexes, $\sum_i n_i K_{a,i}$ (Klotz & Hunston, 1971). In the case of the native protein, data could be fit only for the strong binding site because of the scatter of experimental points at high values of ν. Plots similar in appearance to that of the commercial protein were found for S-ovalbumin and alkaline phosphatase treated protein. As is summarized in Table I, all three of these forms of ovalbumin were found to have a single strong binding site for Mn^{2+}, with K_D ranging from about 5.5×10^{-4} M^{-1} for the native protein to 9.4×10^{-4} M^{-1} for alkaline phosphatase treated ovalbumin. Furthermore, K_D values obtained from linear fitting of the Scatchard plots are within experimental error of those obtained from the type I protein titrations, indicating that the weighted sum of weak metal–protein association constants contributes little more than 10% to the total weighted sum $\sum_i n_i K_{a,i}$ ($\sum_i n_i K_{a,i} \ll K_a$). The Mn^{2+} binding properties of acid phosphatase treated ovalbumin are much different than those of protein forms bearing one or more phosphates. As is shown in Figure 4, types I and II titration data could only be fit for a single type of binding site. From a linear least-squares fit to the data, an average metal–protein site occupancy of about 1.8 is obtained, where the weighted average of metal–protein dissociation constants is at least a factor of 2 greater than the K_D obtained for the native protein.

On comparison of the K_D values (summarized in Table I) for different forms of ovalbumin protein, a trend is obvious between the number of phosphoserines present on the protein and the overall affinity the protein has for binding Mn^{2+}. Alkaline phosphatase treated ovalbumin, which bears only phosphoserine-68, has a significantly lower affinity for Mn^{2+} than does the native protein. Acid phosphatase treated ovalbumin, which lacks both phosphoserines, has the lowest affinity for Mn^{2+} of the three protein forms considered. Calculating free energies of metal–protein association from K_D values, one finds that the change in free energy per phosphate added to the protein ($\delta \Delta G°$) is 0.27 kcal in both cases. The K_D obtained from the Scatchard data for S-ovalbumin does not differ significantly from that obtained for the native protein (although a sight increase is observed in K_D obtained from the type I titration data).

pH Dependence of Mn^{2+} Binding to Ovalbumin. In order to determine the pK_a of the ligands coordinating Mn^{2+}, type I titrations were carried out at several pH values below pH 7.8. Results of these experiments are shown in Figure 5A. Lines in the figure correspond to linear least-squares best fits. Data of pH 5.0 and 6.0 were fit only to the first four and seven data points, since nonlinearity was marked at dilute protein concentrations due to low affinity of metal for the protein under these conditions. Experiments could not be carried out at pH values much above 7.8 due to precipitation in the sample [likely arising from $Mn(OH)_2$ or aggregation of protein–metal complexes]. From linear extrapolation ϵ_b values of 12.5 ± 1.8, 12.9 ± 1.3, 10.5 ± 0.8, and 10.7 ± 0.2 were found at pH 5.0, 6.0, 7.0, and 7.8, respectively. Protein–Mn^{2+} association constants extrapolated from the data of Figure 5A are shown as a function of pH in Figure 5B. The affinity rises expotentially with pH, as would be expected for a titrating group lying much above pH 8. The least-squares best-fit curve to the data was obtained by assuming a Hill coefficient of 0.8 ± 0.07.

Binding of Other Divalent Metals to Ovalbumin. Since one of the suggested functions of ovalbumin is the transportation and storage of metals (Taborsky, 1974), we decided to carry out water PRR enhancement studies with other paramagnetic metal ions. Type I protein titrations were carried out with commercial ovalbumin at fixed concentrations of $CuCl_2$, $CoCl_2$, $GdCl_3$, and $DyCl_3$. These experiments were expeced to yield limited information on the sites of strongest binding. It was found that, under a wide variety of various buffer concentrations and pH values, Cu^{2+} complexes with the protein resulted in precipitation in our samples. This was particularly true at high protein concentrations, making the determination of accurate ϵ_b and K_D values for the Cu^{2+}–ovalbumin complex impossible. It is likely that such precipitation results from aggregation of protein–Cu^{2+} complexes. Similar problems were encountered with Gd^{3+}–protein complexes above pH 6.0 and with Dy^{3+}–protein complexes above pH 7.0. Extrapolation of type I titration data for Gd^{3+} at pH 6.0, Dy^{2+} at pH 7.0, and Co^{2+} at pH 7.8 yielded ϵ_b values of 10.6 ± 0.1, 2.4 ± 0.1, and 6.4 ± 0.9 for the binary protein–Gd^{3+}, –Dy^{3+}, and –Co^{2+} complexes, respectively. Corresponding best-fit dissociation constants for the metal–protein complexes were determined as $(2.47 \pm 0.02) \times 10^{-4}$ M, $(3.71 \pm 0.02) \times 10^{-4}$ M, and $(2.92 \pm 0.54) \times 10^{-3}$ M.

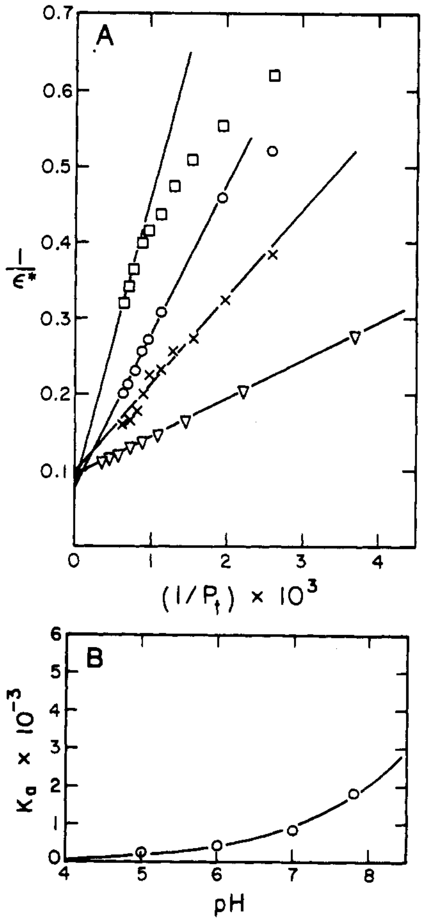

FIGURE 5: (A) Water PRR enhancement data (at 30 °C) for a type I titration of 1.39 mM $MnSO_4$ with chromatographically purified fIII ovalbumin. Experimental data points represent reciprocal enhancements ($1/\epsilon^*$) as a function of reciprocal total protein concentration ($1/P_t$) at pH 5.0 (□), 6.0 (○), 7.0 (×), and 7.8 (▽), in 50 mM Tris buffer. Lines drawn in the figure represent linear least-squares best fits to experimental data points taken at high protein concentrations (greater than 0.5 mM protein). (B) pH dependence of Mn^{2+}–ovalbumin binary association constants extrapolated from the type I titration data of the plot shown in panel A. The enhancements for the bound complex (ϵ_b) in calculating K_a's are summarized in the text.

Vogel & Bridger (1982) found that saturating levels of Mg^{2+} induced changes in chemical shifts of phosphoserine ^{31}P resonances of 0.25–0.32 ppm. On the basis of these shifts Mg^{2+}–protein dissociation constants of 10–20 mM were calculated. Over a wide range of Mn^{2+} to protein ratios we noted no changes in water PRR enhancements when Mg^{2+} was added to ovalbumin samples of pH 7.8. Identical results were obtained when Ca^{2+} was used as the competing metal ion. Hence, if Mg^{2+} and Ca^{2+}, in fact, bind to ovalbumin, it appears

Table II: ^{31}P NMR Relaxation Data and Calculated Correlation Times for Phosphoserine-68 or Alkaline Phosphatase Treated Ovalbumin (pH 7.8, 30 °C)[a]

^{31}P frequency (MHz)	sample conditions	$1/fT_{1P}$ (s^{-1})	$1/fT_{2P}$ (s^{-1})	τ_c (from T_{1P}/T_{2P}) ($\times 10^9$ s)
36.22	2.2 mM protein, 2.2 μM Mn^{2+}	1643 ± 234	17717 ± 6665	16.7 ± 5.0
80.76	2.2 mM protein, 2.2 μM Mn^{2+}	1949 ± 234	83556 ± 23294	15.6 ± 3.2
80.76	2.2 mM protein, 1 μM Mn^{2+}	1767 ± 273	80108 ± 25311	16.2 ± 4.0
121.46	2.2 mM protein, 2.2 μM Mn^{2+}	526 ± 102	80234 ± 4183	19.8 ± 7.3

[a] An error of ±10% was assumed in all T_1 measurements, an error of ±25% was assumed in all T_2 measurements obtained from line width measurements, and an error of ±15% was assumed in all T_2 measurements using the Carr–Purcell–Meiboom–Gill pulse sequence. All T_2 values, other than T_2^0 at 80.76 MHz, were estimated from line widths. T_1 measurements at 121.46 MHz were obtained by the progressive saturation technique. Values of f are based on Mn^{2+}–protein dissociation constants listed in Table I.

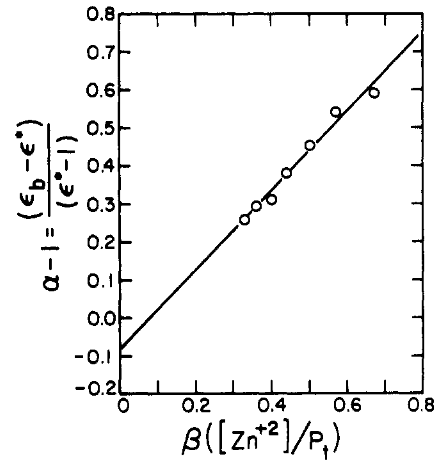

FIGURE 6: Competitive water PRR enhancement data for a type I titration with commercial ovalbumin at pH 7.8 in 50 mM Tris buffer at 30 °C. In the experiment, fixed concentrations of $MnCl_2$ (1.39 mM) and $ZnCl_2$ (0.67 mM) were titrated with protein. The data are plotted according to eq 4, assuming an enhancement for the binary Mn^{2+}–protein complex of 10.68 (Table I). The line in the figure represents a linear least-squares best fit to the experimental data.

that they do not compete for the Mn^{2+} binding site. Competitive binding to ovalbumin was observed between Zn^{2+} and Mn^{2+} ions. In order to calculate the affinity of Zn^{2+} for the single strong Mn^{2+} binding site, water PRR enhancements were measured at fixed concentrations of Zn^{2+} and Mn^{2+} while the total protein concentration was varied in a range where $\nu \simeq 0.5$ (see Figure 4). The data were plotted in the form of eq 4; the ϵ_b value for the Mn^{2+}–protein binary complex given in Table I was used (Figure 6). From a linear least-squares best fit of the data a K_D of (6.12 ± 0.61) × 10^{-3} M was obtained for the Zn^{2+}–protein binary complex. From the ratio of slope to intercept of the best-fit line, it was determined that approximately 8% of the Zn^{2+} is bound to the protein over the range of protein concentrations studied.

Mn^{2+}–Phosphoserine Distances in Ovalbumin Proteins. In order to investigate the structure of native and modified ovalbumin in the vicinity of the phosphoserines, ^{31}P NMR relaxation measurements were undertaken. Distances between metal and phosphoserine can be determined once an estimate of the correlation time, τ_c, characterizing the relaxation between the free electron on the metal and the phosphorus nucleus has been made (see eq 6A). In general, the experimentally measured paramagnetic contribution to the relaxation rates of the phosphorus nucleus, $1/T_{1P}$ and $1/T_{2P}$, depends upon the residence time of the metal in the ligand complex, τ_M, the fraction of total ligand bound to the metal at any time, f, and the relaxation rates arising from the presence of the paramagnetic ion a distance r from the observed nucleus, $1/T_{1M}$ and $1/T_{2M}$ (see eq 6A and 6B). If relaxation rates $1/T_{1P}$ and $1/T_{2P}$ show a field dependence, then T_{1M} and T_{2M} must be equal to or greater than τ_M.

Because the ^{31}P resonances arising from phosphoserines in ovalbumin and S-ovalbumin are only separated by 25 Hz at a ^{31}P resonance frequency of 80.76 MHz, T_{1P} and T_{2P} measurements designed to determine τ_c were carried out on the alkaline phosphatase treated protein, in order to avoid severe overlap of resonances likely to arise when Mn^{2+} is added to the sample. In the calculation of normalized values of T_{1P} and T_{2P}, the Mn^{2+}–protein dissociation constant determined from the water PRR enhancements (Table I) was used. In the case of alkaline phosphatase treated protein, approximately 73% of the Mn^{2+} was bound to the protein at any given time. Table II summarizes the results of these measurements at three different field strengths and also lists values of τ_c calculated from the ratio of T_{1P} and T_{2P} at each field. From the Stokes–Einstein relationship, a protein the size of ovalbumin should have an overall rotational correlation time of about 30 ns at 30 °C (Yguerabide et al., 1970). On this basis, the correlation times calculated from the ratio T_{1P}/T_{2P} seem reasonable, if one assumes some degree of internal mobility of the phosphoserine side chain (Oldfield et al., 1975; Doddrell et al., 1972; Vogel et al., 1982). The calculated values of τ_c listed in Table II also are in reasonable agreement with τ_c values calculated for the phosphoserines of apoovalbumin upon the basis of a diamagnetic relaxation mechanism (8–15 ns) (Vogel et al., 1982; Vogel & Bridger, 1982).

For relaxation of a nucleus in the vicinity of a paramagnetic ion, τ_c is in turn dominated by the smallest of τ_M, the lifetime of the metal–ligand complex, τ_R, the rotational relaxation time, and τ_S, the electron-spin correlation time (James, 1975; Reuben & Cohn, 1970). For most Mn^{2+} macromolecular complexes, τ_S is on the order of 0.5–10 ns and, hence, dominates τ_c (Nowak et al., 1973; Reuben & Cohn, 1970; Lee & Nowak, 1984). If, in fact, the correlation times calculated in Table II are valid, then it must be assumed that τ_S for ovalbumin-bound Mn^{2+} is anomalously long, such that τ_R begins to dominate τ_c. If values of τ_c calculated from the T_{1P}/T_{2P} rates are assumed correct, then at all fields at which results are reported $\omega_I^2\tau_c^2 > 1$ and T_{1M} will depend approximately on the square of the field strength (eq 6). The paramagnetic contribution to the normalized relaxation time, fT_{1P}, should also depend on the square of the field strength, if $T_{1M} > \tau_M$ (eq 5A). As shown by the data in Table II, $1/fT_{1P}$ at 36.22 MHz is within experimental error of $1/fT_{1P}$ at 80.76 MHz. On the other hand, the same relaxation rate decreases by about a factor of 4 on going from the lower two frequencies to 121.46 MHz. There are two explanations for this anomalous field dependence of measured $1/fT_{1P}$ values. Since T_{1M} is predicted to depend on the square of the resonance frequency, assuming the anomalously large values of τ_c calculated, then it is possible that at the lower fields $T_{1M} < \tau_M$, which in turn gives rise to values of $1/T_{1P}$ that are smaller than predicted at lower field strengths. Because $T_{1M} > T_{2M}$ (James,

Table III: Ratios of Calculated and Observed ^{31}P NMR Relaxation Rates at Different Resonance Frequencies for Phosphoserine-68 of Alkaline Phosphatase Treated Ovalbumin[a]

method of obtaining value	$T_{1P}(36)/T_{1P}(121)$	$T_{2P}(36)/T_{2P}(121)$	$T_{1P}(36)/T_{1P}(81)$	$T_{2P}(36)/T_{2P}(81)$	$T_{1P}(81)/T_{1P}(121)$	$T_{2P}(81)/T_{2P}(121)$
exptl	0.34 ± 0.11	6.31 ± 4.74	1.23 ± 0.32	6.07 ± 3.60	0.28 ± 0.09	1.19 ± 0.84
calcd from τ_c given in Table II	0.10 ± 0.06	1.34 ± 0.78	0.25 ± 0.11	1.03 ± 0.46	0.44 ± 0.23	1.40 ± 0.74
calcd by assuming $\tau_c = \tau_S$[b]	0.32 ± 0.01	6.62 ± 0.01	1.27 ± 0.03	3.42 ± 0.01	0.25 ± 0.01	1.95 ± 0.01

[a] Abbreviations used such as $T_{1P}(36)$ refers to T_{1P} measured at 36.22 MHz. Experimentally obtained ratios were taken directly from the data of Table II. Ratios were calculated for 2.2 mM protein samples containing 2.2 μM Mn^{2+}. [b] Calculated by assuming $\tau_c = \tau_S = \tau_v/2B \times 657^2\omega_I^2$ where $\omega_I = 2\pi\nu_0$ and ν_0 is the ^{31}P resonance frequency. A best-fit value of $\tau_v/2B = (3.07 \pm 0.05) \times 10^{-32}$ s^3/rad^2 was used in the calculation.

Table IV: Calculated Best-Fit Mn^{2+}–Phosphate Distances and Correlation Times[a] Based on ^{31}P Relaxation Data of Phosphoserine-68 in Alkaline Phosphatase Treated Ovalbumin

^{31}P frequency (MHz)	sample conditions	τ_c ($=\tau_S$) ($\times 10^9$ s)	$f_1(\tau_c)$ ($\times 10^{10}$)	r (Å)[b]
36.22	2.2 mN protein, 2.2 μM Mn^{2+}	0.69 ± 0.01	20.20 ± 0.28	6.23 ± 0.17
80.76	2.2 mM protein, 2.2 μM Mn^{2+}	3.41 ± 0.06	25.62 ± 0.23	6.30 ± 0.14
80.76	2.2 mM protein, 1 μM Mn^{2+}	3.41 ± 0.06	25.62 ± 0.03	6.41 ± 0.18
121.46	2.2 mM protein, 2.2 μM Mn^{2+}	7.72 ± 0.13	6.48 ± 0.10	6.25 ± 0.22

[a] Calculated by assuming $\tau_c = \tau_S = \tau_v/2B \times 657^2\omega_I^2$ where $\omega_I = 2\pi\nu_0$ and ν_0 is the ^{31}P resonance frequency. A best-fit value of $\tau_v/2B = (3.07 \pm 0.05) \times 10^{-32}$ s^3/rad^2 was used in the calculation. $f_1(\tau_c)$ is the correlation function assuming dipolar relaxation (eq 6A). [b] The average value of r is calculated as 6.29 ± 0.18 Å.

1975; Doddrell et al., 1972), it would be expected that $\tau_M \gg T_{2M}$ and $1/fT_{2P}$ at 36.22 MHz would be approximately equal to $1/fT_{2P}$ at 80.76 MHz. This is seen not to be the case. In fact, $1/fT_{2P}$ at 80.76 MHz is 4–5 times that of the same rate at 36.22 MHz, as would be expected for a ω_I^2 relaxation rate dependence. On this basis, it may be concluded that $T_{2M} > \tau_M$ and, hence, $T_{1M} \gg \tau_M$ (the metal is in fast exchange with the protein ligand).

Table III lists all the possible ratios of measured T_{1P} and T_{2P} values at the three field strengths, as well as those calculated from τ_c values listed in Table II. Even when the large experimental errors in calculated values of τ_c are included, half of the calculated ratios [T_{1P}(36 MHz)/T_{1P}(121 MHz), T_{1P}(36 MHz)/T_{1P}(81 MHz), and T_{2P}(36 MHz)/T_{2P}(81 MHz)] do not agree with those measured experimentally. However, all of these inconsistencies may be removed by assuming that τ_c values calculated from T_{1P}/T_{2P} ratios are incorrect. Similar inconsistencies have been found in the Mn^{2+}–phosphorylated inhibitor–enolase system where τ_c values calculated from T_{1P}/T_{2P} ratios were found to be 2–50 times larger than those estimated from the field dependence of $1/T_{1P}$ relaxation rate of water protons (Nowak et al., 1973). The anomalously high T_{1P}/T_{2P} ratios observed may be due to contact contributions contained in the scalar term of $1/T_{2P}$ (see eq 6B). One approach to obtaining a valid estimate of τ_c is to find a value of τ_c that at least fits the T_{1P} ratios in Table III. However, even if the relatively large errors in the measured ratios are taken into account, no single value of τ_c can be found such that the calculated T_{1P} ratios fit those measured experimentally. On the other hand, a very good fit to measured T_{1P} ratios can be obtained by assuming τ_c is determined by τ_S and τ_S is itself frequency-dependent. An approximate form of the Bloembergen–Morgan expression relating τ_S to frequency (Reuben & Cohn, 1970; Bloembergen & Morgan, 1961) is

$$\tau_S = (\tau_v/2B)\omega_S^2 \qquad (7)$$

where B is a constant containing the resultant spin S and the zero-field splitting of Mn^{2+}, τ_v is the characteristic time for symmetry distortions of the complex, and ω_S is $657\omega_I$. A best fit to the T_{1P} ratios was obtained by using $\tau_v/2B = (3.07 \pm 0.05) \times 10^{-32}$ s^3/rad^2. As is shown by the last line in Table III, the assumption of a field dependence of τ_c also leads to a good fit of the measured T_{2P} ratios. In addition, our best-fit value of $\tau_v/2B$ is similar in magnitude to the same ratio obtained from water proton relaxation measurements of the binary Mn^{2+}–pyruvate kinase complex (Reuben & Cohn, 1970).

A list of τ_c values calculated according to eq 7, using the best-fit value of $\tau_v/2B$, are listed in Table IV. These values fall well within the range of τ_c values calculated for other Mn^{2+} macromolecular complexes (Nowak et al., 1973; Reuben & Cohn, 1970; Lee & Nowak, 1984). Distances from the phosphorus of phosphoserine-68 were calculated from these values by using eq 6A and the T_{1M} values listed in Table II. Independent of the experiment carried out, calculated Mn^{2+}–phosphate distances are within experimental error of one another. An average distance of 6.29 ± 0.18 Å is calculated.

One set of ^{31}P NMR relaxation experiments was carried out on native ovalbumin and S-ovalbumin at 80.76 MHz. The Mn^{2+} concentration was carefully adjusted so that a definite rate enhancement could be observed without significant overlap of the ^{31}P resonances arising from phosphoserine-68 and -344. Results of these measurements are summarized in Table V. Values of τ_c calculated from T_{1P}/T_{2P} ratios are anomalously large but quite close to τ_c values calculated for the alkaline phosphatase treated protein by using the same method of calculation (Table II). Because of the problems inherent in this method of calculation of τ_c, τ_c values used in the calculation of Mn^{2+}–phosphate distances were assumed to be the same as those found for the alkaline phosphatase treated protein, having assumed a frequency dependence in τ_c. It is seen that the Mn^{2+}–phosphate distance to phosphoserine-68 in the native protein is within experimental error of the same calculated distance in the alkaline phosphatase treated protein. On the other hand, phosphoserine-344 is calculated to be about 0.8 Å closer than phosphoserine-68 to the Mn^{2+} center. The results summarized in Table V also indicate that when ovalbumin is converted to the S form of the protein phosphoserines-68 and -344 move about 1.0 and 0.5 Å, respectively, farther away from the metal ion center.

Role of Oligosaccharide in Mn^{2+} Binding to Ovalbumin. In order to determine what effect, if any, the single oligosaccharide chain attached to ovalbumin has upon Mn^{2+} binding, type I titrations were carried out on ovalbumin treated with α-mannosidase and β-*N*-acetylglusaminidase. Reference to the primary carbohydrate sequence of the oligosaccharide shows that such treatment is likely to remove the nonreducing

Table V: ^{31}P Relaxation Data and Calculated Phosphoserine–Mn^{2+} Distances for Commercial Ovalbumin and S-Ovalbumin Prepared from the Commercial Protein (30 °C, pH 7.8)[a]

obsd ^{31}P resonance	$1/fT_{1P}$ (s^{-1})	$1/fT_{2P}$ (s^{-1})	τ_c (from T_{1P}/T_{2P}) ($\times 10^9$ s)	r (Å)[b]
commercial ovalbumin				
P-Ser-68	2839 ± 686	67 735 ± 18 158	12.0 ± 3.2	5.95 ± 0.26
P-Ser-344	5491 ± 1154	111 665 ± 20 560	10.8 ± 2.3	5.31 ± 0.20
S-ovalbumin				
P-Ser-68	1075 ± 269	31 718 ± 8568	13.3 ± 3.6	6.99 ± 0.30
P-Ser-344	3338 ± 291	71 098 ± 13 328	19.0 ± 4.2	5.75 ± 0.10

[a] All ^{31}P NMR spectra were acquired at 80.71 MHz by using unbuffered protein solutions (20% D_2O). Samples of ovalbumin and S-ovalbumin in the absence of added metal were 1.9 and 2.2 mM, respectively. Protein samples with metal added had total protein concentrations of 2.4 mM. Mn^{2+} was added to commercial ovalbumin and S-ovalbumin samples to give total final Mn^{2+} concentrations of 0.6 and 1.7 μM, respectively. Relaxation measurements were made by using inversion–recovery and CPMG techniques. An error of ±15% was assumed in measured relaxation rates. [b] Distances were calculated by assuming $\tau_c = \tau_S = 3.41 \pm 0.06$ ns, as was calculated for alkaline phosphatase treated ovalbumin.

terminal *N*-acetylglucosamine β-1,4-linked to mannose and terminal α-1,3- and α-1,6-linked mannose residues. Following exhaustive enzymatic treatment, it was found that a total of 0.8 hexose was removed from the protein. This modified protein has Mn^{2+} binding characteristics identical with those of native commercial ovalbumin, as determined by a type I titration. In order to determine the proximity of the nonreducing end of the ovalbumin oligosaccharide chain to the metal ion binding sites on ovalbumin and S-ovalbumin, [1-^{13}C]-galactose was attached to the nonreducing terminal *N*-acetylglucosamine residue of the chain according to the procedure previously described (Goux et al., 1982). However, stoichiometric quantities of Mn^{2+} added to these two forms of the protein failed to produce any detectable change in relaxation times of the ^{13}C nucleus. If it is assumed a T_1 can be measured for the protein in the presence of Mn^{2+} that differs from the T_1 of the apoprotein by at least 10%, then a lower limit to the Mn^{2+}–^{13}C-labeled galactose distance of about 40 Å is calculated.

DISCUSSION

Ovalbumin from egg white was one of the very first proteins isolated and crystallized in pure form [for a review, see Taborsky (1974)]. Becuase it is a complex protein, bearing two covalently linked phosphates and a single oligosaccharide chain, it has most often been used as a "model" for investigations of phosphorylated proteins and simple glycoproteins. Although its functional significance is unknown, it was long ago suggested that the protein might serve to transport or store metal ions. It is quite surprising that, throughout all of the hypothesizing, thorough metal ion binding studies on ovalbumin have never been undertaken. Using water proton relaxation rate enhancement by paramagnetic metal ions, we have obtained data which indicate that ovalbumin indeed binds a variety of di- and trivalent metal ions (including Mn^{2+}, Co^{2+}, Cu^{2+}, Zn^{2+}, Gd^{3+}, and Dy^{3+}) at a single binding site on the protein. Numerous secondary binding sites for these metals also exist on ovalbumin that have affinities for these metal ions at least 1 order of magnitude less than that of the single strong binding site. On the basis of competitive water PRR enhancement studies, neither Mg^{2+} nor Ca^{2+} appears to displace Mn^{2+} from the strong binding site. These results for Mg^{2+} binding are in reasonable agreement with previous results indicating that binding of Mg^{2+} to the protein at pH 8.3 is weak [(10–20 × 10^{-3} M] (Vogel & Bridger, 1982). Water PRR enhancement studies using Co^{2+}, Gd^{2+}, and Dy^{3+} as relaxation probes were undertaken primarily to determine the effect of ionic size and charge on binding to the single strong binding site on ovalbumin. The lower affinity of Co^{2+} for this site compared to that of Mn^{2+} is consistent with limited steric access to the binding site. On the other hand, an increase in ionic charge more than compensates for the size effect, as is evidenced by the higher affinity that Gd^{3+} and Dy^{3+} have for the binding site when compared to that of Mn^{2+}. In the latter case, one would expect, on the basis of the pH dependence of the Mn^{2+}–protein binding constant, that had it been possible to study trivalent ion binding under conditions similar to those used in Mn^{2+} binding studies (pH 7.8), the difference in binding constants between di- and trivalent ions would have been even more pronounced (Figure 5B).

Not surprising is the role of phosphoserines in metal ion binding. Phosvitin, a protein component of egg yolk that has nearly all of its serines phosphorylated, is known to bind iron in the stoichiometric ratio 1:2 Fe^{3+}:phosphoserine (Taborsky, 1963). It is interesting that the same metal:phosphoserine stoichiometry, 1:2 Mn^{2+}–phosphoserine, is observed in native ovalbumin. More detailed spectroscopic and magnetic studies on phosvitin yielded results that were consistent with a tetrahedrally structured polynuclear complex in which oxygen ligands are provided by appropriately spaced phosphate groups, possibly attached to parallel chains of the protein ordered in a β-type structure (Webb et al., 1973). A similar metal ion–ovalbumin complex is consistent with the decreased affinity of the protein for Mn^{2+} when one or more of the phosphates are cleaved from ovalbumin by phosphatases (Table II). However, as will be discussed below, if such a complex involving the two phosphoserines of ovalbumin exists, it is unlikely it involves direct coordination of phosphate oxygens without the presence of intervening water molecules. Furthermore, our results indicating that ovalbumin bearing no phosphoserine (acid phosphatase treated) is able to bind two Mn^{2+} ions (although with one-fourth the affinity for each) suggest that other groups on the protein act as ligands. Phosvitin also forms precipitable complexes with Ca^{2+} and Mg^{2+} (McIndoe, 1961), a condition reminiscent of that observed upon adding Cu^{2+} to concentrated ovalbumin samples. It may be the case that Cu^{2+} produced such effects in ovalbumin by forming intermolecular phosphate–Cu^{2+}–phosphate complexes leading to protein aggregation and precipitation.

Several of the results that we obtained in our study give clues as to the structural environment of the Mn^{2+} ion binding site on ovalbumin. When the pH titration of the phosphoserines was carried out by ^{31}P NMR, it was determined that the pK_a of phosphoserine-68 in native ovalbumin was significantly higher than in alkaline phosphatase treated ovalbumin, in which phosphoserine-344 was enzymatically removed (pK_a's of about 6.2 and 5.6, respectively). This result seems to indicate that in the native protein the side chain of phosphoserine-344 is near enough to the phosphate of phosphoserine-68 so as to indirectly influence its titration behavior. On the basis of paramagnetic relaxation of phosphorus nuclei in alkaline phosphatase treated and native ovalbumin, it was determined that the Mn^{2+} ion binds at distances of 6.0–6.5 Å from phosphoserine-68 and 5.1–5.5 Å from phosphoserine-344, respectively. Both of these distances fall well within the range determined by ^{31}P NMR relaxation measurements for other Mn^{2+} to enzyme-phosphate-containing complexes, where the phosphate lies in the second coordination sphere of the metal (4.9–6.5 Å) (Nowak et al., 1973; Lee & Nowak, 1984; Mildvan, 1977). On the basis of a comparison of these distances with those expected for a Mn^{2+}–phosphate coordination complex, it has been proposed that in the former case a water molecule intervenes between the metal and the phosphate group. However, because acid phosphatase treated ovalbumin (with both phosphates removed from the protein) appears to bind Mn^{2+}, it is likely that other groups in the near vicinity of the phosphoserines also act as ligands. Reference to the primary sequence of the protein shows that aspartic acid immediately precedes phosphoserine-68 from the N-terminal and glutamic acid occurs as the $n + 2$ residue for both phosphoserines (Nisbet et al., 1981; McReynolds et al., 1978). It is quite possible that carboxylate side chains from these residues also act as Mn^{2+} ligands. In this respect, the pH dependence of the Mn^{2+}–protein binding constant appears confusing. Figure 5B presents data which, at least, suggest that the primary Mn^{2+} ligand has a pK_a significantly above 8.0. Likely possibilities include tyrosine or lysine side chains.

The exact nature of the changes in ovalbumin conformation brough about by conversion to the S form of the protein is unclear. Optical activity and hydrodynamic studies indicate that S-ovalbumin has a more compact conformation with a higher percentage of α-helical residues than does the native protein (Smith & Black, 1968a,b). On the other hand, Raman spectral studies suggest that there is a loss of α-helical structure in favor of antiparallel β-pleated sheet structure when native protein is converted to the S form (Kint & Tomimatsu, 1979). On the basis of ^{31}P NMR relaxation studies carried out at high pH, we conclude that there is a 0.5–1.0-Å lengthening of both Mn^{2+}–phosphate distances upon conversion of native protein to S-ovalbumin (Tables III and IV). In this respect, the "looser" Mn^{2+}–phosphoserine complex in S-ovalbumin may manifest itself in the form of the weaker affinity that Mn^{2+} seems to have for this altered form of the protein (Table I).

In a number of cases, the oligosaccharide chains attached to glycoproteins appear to influence enzyme activity or protein conformation (Tanner, 1978; Komoda & Sakagishi, 1978, 1976). In this study we find that treatment of ovalbumin with glycosidases had no effect on the affinity of the protein for Mn^{2+} ion. Furthermore, no changes in relaxation rates of the ^{13}C nucleus of [1-^{13}C]galactose enzymatically attached to the nonreducing terminal of the oligosaccharide chain were seen upon adding Mn^{2+} to protein solutions in stoichiometric amounts. One must conclude from these data that at least the nonreducing terminal end of the oligosaccharide chain is quite distant from the Mn^{2+} ion binding site on the protein. This results is in qualitative agreement with the large degree of internal mobility the terminal end of the carbohydrate was found to have, on the basis of diamagnetic relaxation models (Goux et al., 1982). In order to study the effect that protein conformation has on the Mn^{2+}–carbohydrate distances, one must at the very least have a protein system where the resonance signal of interest arising from the attached oligosaccharide is within 15 Å or so of the Mn^{2+} ion binding site on the protein. This appears not to be the case for either ovalbumin or S-ovalbumin. Future studies along these lines will be directed toward metal ion binding proteins or enzymes where attached oligosaccharide chains lie in the vicinity of the active site or metal ion binding site.

Registry No. Mn, 7439-96-5; phosphoserine, 407-41-0.

REFERENCES

Atkinson, P. H., Grey, A., Carver, J. P., Hakimi, J., & Ceccarini, C. (1981) *Biochemistry 20*, 3979–3986.

Berman, E., Walters, D. E., & Allerhand, A. (1981) *J. Biol. Chem. 256*, 3853–3857.

Bloembergen, N. (1957) *J. Chem. Phys. 27*, 572–573.

Bloembergen, N., & Morgan, L. O. (1961) *J. Chem. Phys. 34*, 842.

Carr, H. Y., & Purcell, E. M. (1954) *Phys. Rev. 94*, 630–638.

Doddrell, D., Glushko, V., & Allerhand, A. (1972) *J. Chem. Phys. 56*, 3683–3689.

Donovan, J. W., & Mapes, C. J. (1976) *J. Sci. Food Agric. 27*, 197–204.

Dubois, M., Giles, K. A., Hamilton, J. K., Rebers, P.A., & Smith, F. (1956) *Anal. Chem. 28*, 350–354.

Freeman, R., & Hill, H. D. W. (1971) *J. Chem. Phys. 54*, 3367–3377.

Glasoe, P. K., & Long, F. A. (1960) *J. Phys. Chem. 64*, 188–190.

Goux, W. J., Perry, C., & James, T. L. (1982) *J. Biol. Chem. 257*, 1829–1835.

Granot, J., & Kearns, D. R. (1982) *Biopolymers 21*, 203–218.

James, T. L. (1975) in *Nuclear Magnetic Resonance in Biochemistry*, Chapter 6, Academic Press, New York.

Kint, S., & Tomimatsu, Y. (1979) *Biopolymers 18*, 1073–1079.

Klotz, I. M., & Hunston, D. L. (1971) *Biochemistry 10*, 3065–3069

Komoda, T., & Sakagishi, Y. (1976) *Biochim. Biophys. Acta 445*, 645–660.

Komoda, T., & Sakagishi, Y. (1978) *Biochim. Biophys. Acta 523*, 395–406.

Lee, M. H., & Nowak, T. (1984) *Biochemistry 23*, 6506–6513.

Linderstrom-Lang, K., & Ottesen, M. (1949) *C. R. Trav. Lab. Carlsberg 26*, 403.

Luz, Z., & Meiboom, S. (1964) *J. Chem. Phys. 40*, 2686–2692.

McIndoe, W. M. (1961) *Biochem. J. 80*, 418.

McReynolds, L., O'Malley, B. W., Nisbet, A. D., Fothergill, J. E., Giuol, D., Fields, S., Robertson, M., & Brownlee, G. G. (1979) *Nature (London) 273*, 723–728.

Meiboom, S., & Gill, D. (1958) *Rev. Sci. Instrum. 29*, 688–691.

Mildvan, A. S. (1977) *Acc. Chem. Res. 10*, 246–262.

Mildvan, A. S., & Cohn, M. (1963) *Biochemistry 2*, 910–919.

Nakamura, R., & Masuko, I. (1981) *Agric. Biol. Chem. 45*, 2775–2780.

Nakamura, R., Hirai, M., & Takemori, Y. (1980) *Agric. Biol. Chem. 44*, 149–153.

Nakamura, R., Takemori, Y., & Shitamori, S. (1981) *Agric. Biol. Chem. 45*, 1653–1659.

Narashiman, S., Harpaz, N., Longmore, G., Carver, J. P., Grey, A., & Schachter, H. (1980) *J. Biol. Chem. 255*, 4876–4884.

Nisbet, A. D., Saundry, R. H., Moir, A. J., Fothergill, L. A., & Fothergill, J. E. (1981) *Eur. J. Biochem. 115*, 335–345.

Norton, R. S., & Allerhand, A. (1977) *J. Biol. Chem. 252*, 1795–1798.

Nowak, T., Mildvan, A. S., & Kenyon, G. L. (1973) *Biochemistry 12*, 1690–1701.

Oldfield, E., Norton, R. S., & Allerhand, A. (1975) *J. Biol. Chem. 250*, 6368–6380.

Reuben, J., & Cohn, M. (1970) *J. Biol. Chem. 245*, 6539–6546.

Rhodes, M. B., Azari, P. R., & Feeney, R. E. (1958) *J. Biol. Chem. 230*, 399–408.

Scatchard, G. (1949) *Ann. N.Y. Acad. Sci. 51*, 660–672.

Smith, M. B., & Black, J. F. (1968a) *Aust. J. Biol. Sci. 21*, 539–548.

Smith, M. B., & Black, J. F. (1968b) *Aust. J. Biol. Sci. 21*, 549–558.

Solomon, I. (1955) *Phys. Rev. 99*, 559–565.

Swift, T. J., & Connick, R. E. (1962) *J. Chem. Phys. 37*, 307–320.

Taborsky, G. (1963) *Biochemistry 2*, 266.

Taborsky, G. (1974) *Adv. Protein Chem. 28*, 1–187.

Tai, T., Yamashita, K., Ogata-Arakawa, M., Koide, N., Muramatsu, T., Iwashita, S., Iwove, Y., & Kobada, A. (1975) *J. Biol. Chem. 250*, 8569–8576.

Tamimatsu, Y. (1965) *Biochim. Biophys. Acta 94*, 525–534.

Tanner, M. J. A. (1978) in *Current Topics in Membranes and Transport* (Bronner, F., & Kleinziller, A., Eds.) Vol. 11, pp 279–325, Academic Press, New York.

Vogel, H. J., & Bridger, W. A. (1982) *Biochemistry 21*, 5825–5831.

Vogel, H. J., Bridger, W. A., & Sykes, B. D. (1982) *Biochemistry 21*, 1126–1132.

Vold, R. L., Waugh, J. S., Klein, M. P., & Phelps, D. E. (1968) *J. Chem. Phys. 48*, 3831–3832.

Webb, J., Multani, J. S., Saltman, P., Beach, N. A., & Gray, H. B. (1973) *Biochemistry 12*, 1797.

Yguerabide, J., Epstein, H. F., & Stryer, L. (1970) *J. Mol. Biol. 51*, 573–590.

Kinetic Analysis by Stopped-Flow Radiationless Energy Transfer Studies: Effect of Anions on the Activity of Carboxypeptidase A[†]

Angela C. Williams and David S. Auld*

Center for Biochemical and Biophysical Sciences and Medicine and Department of Pathology, Harvard Medical School, and Brigham and Women's Hospital, Boston, Massachusetts 02115

Received July 29, 1985

ABSTRACT: We have utilized a highly sensitive radiationless energy transfer (RET) assay to investigate the effect of anions on the activity of carboxypeptidase A (CPD-A). The RET kinetic method visualizes the ES complex directly and thus enables both the mode of action of anions and the quantitation of their effect to be determined at a single substrate concentration. In marked contrast to the activating effect of anions on the closely related metalloprotease, angiotensin converting enzyme, Cl^-, and other anions inhibit CPD-A catalysis. NaCl inhibits the hydrolysis of Dns-Ala-Ala-Phe throughout the pH range 6–10. Other di- and tripeptides are similarly inhibited while their ester analogues are affected only slightly. Changes in the type of cation [e.g., Na^+, Li^+, K^+, Ca^{2+}, and $(CH_3)_4N^+$] at a constant [Cl^-] of 0.1 M showed no difference in the extent of inhibition, whereas with anion substitution the differences were marked. In all cases, the inhibition was partially competitive. At pH 5.9, the K_i values for the free enzyme are 51 (Cl^-), 17 (N_3^-), 2.1 (SO_4^{2-}), and 0.21 mM ($H_2PO_4^-$), and for the ES complex, the K_I' values are 1000, 720, 42, and 13 mM, respectively. The other anions were shown to act at the chloride site. The results indicate that investigations of anion inhibition in 1 M NaCl, a typical assay condition, may be greatly hindered by the presence of Cl^-. Thus, the competitive binding mode of phenylacetate toward peptide hydrolysis is greatly decreased by the presence of 1 M Cl^- ion while its noncompetitive component is unaffected. The site of anion interaction is not likely the metal atom since spectroscopic studies have indicated that binding to this site is much weaker than is observed here. Since Cl^- and PO_4^{2-} can decrease the rate of inactivation of the enzyme by butanedione, an arginine residue is a likely anion binding site. The results of the study are discussed in terms of the effect of salt on the solubility of the enzyme and the reduced catalytic activity of the crystals.

The active site of carboxypeptidase A contains several cationic groups (Arg-145, -127, -124, and -71 and Zn^{2+}). Its substrates, which are carboxylates, and some of its most potent inhibitors, such as β-phenylpropionate (Kaufman & Neurath, 1949) and benzyl succinate (Palmer et al., 1982), are known to be negatively charged. Until now, it has been impossible to evaluate the effect of anions on the enzyme's activity because it is generally assayed in 0.5–1 M NaCl due to its limited solubility in the absence of NaCl. We have now used a highly sensitive radiationless energy transfer (RET)[1] assay to overcome the problem. The RET assay was used in this study because it provides a means of observing submicromolar concentrations of enzyme–substrate complexes and greatly simplifies analysis of modifier effects (Auld et al., 1972, 1977).

[†] This work was supported by Grant-in-Aid GM-24967 from the National Institutes of Health, Department of Health and Human Services, to Harvard Medical School.

* Correspondence should be addressed to this author at the Center for Biochemical and Biophysical Sciences and Medicine, Harvard Medical School.

[1] Abbreviations: CPD-A, carboxypeptidase A; ACE, angiotensin converting enzyme; RET, radiationless energy transfer; ammediol, 2-amino-2-methyl-1,3-propanediol; Mes, 2-(*N*-morpholino)ethanesulfonic acid; Hepes, *N*-(2-hydroxyethyl)piperazine-*N'*-2-ethanesulfonic acid; Dns, dansyl [5-(dimethylamino)naphthalene-1-sulfonyl]; Tris, tris(hydroxymethyl)aminomethane; OPhe, L-β-phenyllactate.

0006-2960/86/0425-0094$01.50/0